Henson, Stephanie; Yool, Andrew; Sanders, Richard. 2015 Variability in efficiency of particulate organic carbon export: A model study. *Global Biogeochemical Cycles*, 29 (1). 33-45. 10.1002/2014GB004965

Henson, Stephanie; Yool, Andrew; Sanders, Richard. 2015 Variability in efficiency of particulate organic carbon export: A model study. *Global Biogeochemical Cycles*, 29 (1). 33-45. 10.1002/2014GB004965

AGU PUBLICATIONS

Global Biogeochemical Cycles

RESEARCH ARTICLE
10.1002/2014GB004965

Key Points:
- Seasonal and spatial variability in export ratio quantified
- Empirical algorithms for e-ratio may be overly simple
- Assuming e-ratio is seasonally invariant results in large errors in export

Correspondence to:
S. A. Henson,
S.Henson@noc.ac.uk

Citation:
Henson, S. A., A. Yool, and R. Sanders (2015), Variability in efficiency of particulate organic carbon export: A model study, *Global Biogeochem. Cycles*, *29*, 33–45, doi:10.1002/2014GB004965.

Received 11 AUG 2014
Accepted 8 DEC 2014
Accepted article online 11 DEC 2014
Published online 9 JAN 2015

Variability in efficiency of particulate organic carbon export: A model study

Stephanie A. Henson[1], Andrew Yool[1], and Richard Sanders[1]

[1]National Oceanography Centre, Southampton, UK

Abstract The flux of organic carbon from the surface ocean to mesopelagic depths is a key component of the global carbon cycle and is ultimately derived from primary production (PP) by phytoplankton. Only a small fraction of organic carbon produced by PP is exported from the upper ocean, referred to as the export efficiency (herein e-ratio). Limited observations of the e-ratio are available, and there is thus considerable interest in using remotely sensed parameters such as sea surface temperature to extrapolate local estimates to global annual export flux. Currently, there are large discrepancies between export estimates derived in this way; one possible explanation is spatial or temporal sampling bias in the observations. Here we examine global patterns in the spatial and seasonal variability in e-ratio and the subsequent effect on export estimates using a high-resolution global biogeochemical model. The model used here represents export as separate slow- and fast-sinking detrital material whose remineralization is respectively temperature dependent and a function of ballasting minerals. We find that both temperature and the fraction of export carried by slow-sinking particles are factors in determining e-ratio, suggesting that current empirical algorithms for e-ratio that only consider temperature are overly simple. We quantify the temporal lag between PP and export, which is greatest in regions of strong variability in PP where seasonal decoupling can result in large e-ratio variability. Extrapolating global export estimates from instantaneous measurements of e-ratio is strongly affected by seasonal variability and can result in errors in estimated export of up to ±60%.

1. Introduction

The oceans are an important sink for atmospheric CO_2 [*Le Quere et al*., 2013] and represent the largest active reservoir of planetary inorganic carbon [*Raven and Falkowski*, 1999]. One route for carbon to enter the ocean is via the biological carbon pump, which is driven by the sinking of organic particles from the upper ocean [*Falkowski et al*., 1998; *Sabine et al*., 2004]. These particles derive ultimately from primary production (PP) by phytoplankton which produce particulate organic carbon (POC), of which the majority is remineralized by metabolic processes in the upper ocean. A fraction, however, survives and is exported into the mesopelagic zone (100–1000 m depth). Quantifying the efficiency with which carbon is transferred out of the upper ocean is thus an important element of understanding the global carbon cycle as it partly sets the air-sea partitioning of CO_2 [*Kwon et al*., 2009].

The fraction of PP that sinks out of the surface ocean is referred to as the export efficiency or export ratio (e-ratio = export / PP). Obtaining an in situ estimate of the e-ratio is challenging as PP and carbon export must be measured simultaneously. There is thus interest in developing simple empirical algorithms relating the e-ratio to remotely sensed parameters, with the goal of providing global, spatially resolved estimates of the organic carbon export flux. Generally, these have been derived from relatively small in situ data sets of export and are parameterized as functions of sea surface temperature (SST), PP, and/or chlorophyll [e.g., *Laws et al*., 2000; *Dunne et al*., 2005; *Henson et al*., 2011].

Currently, export flux is typically estimated using the thorium depletion method [*Buesseler*, 1998] or neutrally buoyant sediment traps [*Lampitt et al*., 2008; *Owens et al*., 2013]. Isotope tracer methods rely on radiogenic daughter products of naturally occurring isotopes which adhere to particulate matter, e.g., ^{234}Th or ^{210}Po. As these sink, a disequilibrium between the parent and daughter isotopes is established, which can be related to carbon export through application of a measured POC:isotope activity ratio. These methods have integration time scales related to the half-life of the daughter isotope and range from ~ 24 days for ^{234}Th to ~ 4.5 months for ^{210}Po. Neutrally buoyant sediment traps are typically of a similar construction

to conventional moored sediment traps but are designed to be free drifting at predetermined depths. Samples of sinking material are collected in cups and analyzed for POC content. These types of sediment traps are usually deployed for ~0.5–5 days. The e-ratio estimates thus derived are necessarily quasi-instantaneous, with the integration time scale dependent on the method used. Nevertheless, these measurements are used to derive algorithms to estimate the annual total carbon exported. This extrapolation implicitly assumes that the e-ratio does not change substantially during the course of a year so that the instantaneous e-ratio estimate represents the annual mean e-ratio and can thus be applied to annual total PP to obtain annual total export (as done in, e.g., *Henson et al*. [2011] and *Laws et al*. [2000]). However, observational studies that have repeatedly sampled the same location have demonstrated that the e-ratio can vary seasonally. In high-latitude regions, the e-ratio is generally observed to increase from spring to summer [*Baumann et al*., 2013; *Kawakami and Honda*, 2007; *Buesseler et al*., 1992], while at low latitudes the e-ratio is relatively constant [*Brix et al*., 2006; *Benitez-Nelson et al*., 2001], although high e-ratios are occasionally observed during periods of very low PP at Bermuda Atlantic Time-series Study (BATS) [*Buesseler*, 1998]. Overall, the limited number of seasonally resolved studies suggests that intraannual variability in e-ratio does occur, with the degree of variability dependent on location.

A related issue is that of a time lag between PP and subsequent export. This "decoupling" between PP and export is generally recognized, although the limitations of in situ sampling make it difficult to quantify, and occasionally e-ratios exceeding 1 are reported, implying that more carbon is exported than is produced. In both low-latitude and high-latitude regions [e.g., *Buesseler*, 1998; *Benitez-Nelson et al*., 2001; *Buesseler et al*., 2009; *Moran et al*., 2012; *Baumann et al*., 2013], lags between PP and export have been noted and ascribed to the seasonal development of the food web, such that at the start of the productive period, PP increases rapidly, but the resultant export may not occur immediately due to the time required for processing of carbon in the upper ocean via, for example, zooplankton grazing, resulting in apparently low e-ratio. Following the same argument, e-ratios greater than 1 likely occur at the end of the productive period, when PP is decreasing but export, originating from the standing stock of biomass, may still be ongoing.

Here we use a medium complexity global biogeochemical model to investigate spatial and seasonal variability in e-ratio. The model proves to be a useful tool to investigate how the lag between PP and export leads to a nonuniform e-ratio which may affect how we interpret sparse in situ data. Further, we investigate the implications for estimates of global carbon export derived from limited observations.

2. Methods

In this study, we use the global Nucleus for European Modeling of the Ocean (NEMO) ocean general circulation model coupled to the plankton ecosystem model Model of Ecosystem Dynamics, carbon Utilization, Sequestration, and Acidification (MEDUSA) [*Yool et al*., 2011]. The version of NEMO used here is v3.2 and has a horizontal resolution of ¼° and a vertical resolution of 64 levels. In the top 100 m, there are 14 levels increasing from 6 m in thickness at the surface to 10 m at 100 m depth. NEMO surface forcing uses the DFS4.1 fields developed by the European DRAKKAR collaboration [*DRAKKAR Group*, 2007], which combines the Common Ocean-ice Reference Experiment data set [*Large and Yeager*, 2004] with the ERA-40 reanalysis.

MEDUSA is a medium complexity model that simulates the cycles of nitrogen, silicon, and iron. The model divides the plankton community into "small" and "large" fractions, where the small portion of the ecosystem represents the microbial loop of picophytoplankton and microzooplankton. The large fraction represents microphytoplankton (diatoms) and mesozooplankton. As such, MEDUSA represents separately small, fast-growing phytoplankton controlled by fast-growing microzooplankton, and large, slower-growing phytoplankton that can temporarily evade the control of slower-growing mesozooplankton, and which therefore can form phytoplankton blooms. The nonliving particulate detritus is also split between small, slow-sinking particles and large, fast-sinking particles. Small particles sink out of the upper ocean at a rate of 3 m d^{-1} and are remineralized at a rate dependent on temperature:

$$R = \mu_D \cdot 1.066^T \cdot D$$

where T is temperature, D is slow-sinking detritus (mmol N m^{-3}), and μ_D is the detrital nitrogen remineralization rate at 0°C (0.016 day^{-1}). This form results in faster recycling of detritus in warm waters driven by bacteria in

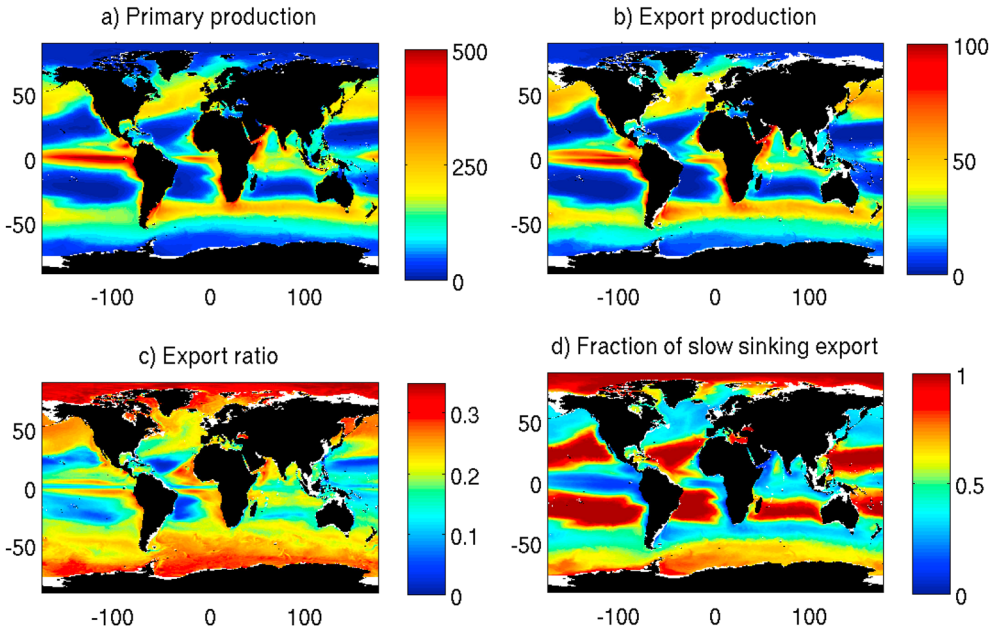

Figure 1. Annual total modeled (a) primary production and (b) export production (g C m^{-2}); annual mean modeled (c) export ratio and (d) fraction of total export in the slow-sinking pool.

the microbial loop, which are not explicitly modeled. Small particles are generated principally by the small fraction of the phytoplankton community (although a minor fraction of the diatom losses also appears in the small detritus) and are consumed by both microzooplankton and mesozooplankton. Large sinking particles are assumed to sink more rapidly than the time step of the model can explicitly resolve so instead are treated implicitly and added to (via production) and depleted (via remineralization) at each level in the water column instantaneously. Large particles are generated by losses of diatoms and mesozooplankton and are remineralized following the ballast model of *Armstrong et al.* [2002], as implemented by *Dunne et al.* [2007], which resolves both organic and mineral fractions of sinking material. A portion of the organic matter is assumed to be associated with the mineral fraction and is protected from remineralization, while the remainder is remineralized following a standard exponential function with depth. The mineral fraction (opal and calcium carbonate) is exponentially diminished by dissolution down the water column, so the amount of protected organic material declines with depth.

An initial physics-only spin-up simulated the period 1978 to 1987 (10 years). The biogeochemistry was then coupled, and MEDUSA was run for the period 1988 to 2007 (20 years). In our analysis, we use the climatological model year averaged over 1995 to 2006 at a 5 day time step. PP is integrated over the full model depth; carbon export is the flux across the 100 m horizon (slow + fast sinking); and the e-ratio is simply export/PP. Full details of the model formulation and validation (at 1° resolution) can be found in *Yool et al.* [2011].

Figure 1 shows annual modeled total PP, export production, e-ratio, and the fraction of total export that is slowly sinking. Modeled globally integrated PP is 44 Pg C yr^{-1}, slightly lower than satellite-derived estimates which range from 46 to 59 Pg C yr^{-1} [*Behrenfeld and Falkowski*, 1997; *Carr et al.*, 2006; *Westberry et al.*, 2008]. Modeled PP is underestimated relative to satellite estimates in the subtropical gyres and overestimated in the Southern Ocean and equatorial Pacific. Globally integrated export flux is 8.5 Pg C yr^{-1}, centered in the range of satellite-derived estimates of 5–12 Pg C yr^{-1} [*Henson et al.*, 2011, and references therein]. The spatial distribution of modeled export has similar patterns to satellite-derived estimates [*Laws et al.*, 2000; *Lutz et al.*, 2007; *Henson et al.*, 2011], although it should be noted that these vary widely. Regardless of which satellite estimate is used, the model consistently overestimates export production in a band at 50°S at the southern edge of the oligotrophic gyres but is otherwise within the range of other estimates. The global mean modeled e-ratio is 0.22, which is close to the median value of global e-ratios (0.19) derived from satellite-based estimates [from *Laws et al.*, 2000; *Dunne et al.*, 2007; *Henson et al.*, 2011; *Siegel et al.*, 2014]. Generally, the model tends

to overestimate the e-ratio in the southerly Southern Ocean and in equatorial upwelling regions, relative to satellite-derived estimates. This is consistent with the comparison to in situ estimates of e-ratio, which vary spatially from ~ 0.01 in the equatorial Pacific to ~ 0.1 at BATS and up to ~ 0.35–0.45 at North Atlantic Bloom Experiment (NABE) and in the Southern Ocean [*Buesseler*, 1998; *Buesseler and Boyd*, 2009]. Where e-ratio is low, the model tends to overestimate e-ratio, e.g., in the equatorial Pacific upwelling, and vice versa in regions of high e-ratio. It should be noted, however, that in situ estimates tend to be from single cruises, whereas Figure 1 shows the model annual average e-ratio. Finally, an important point to note is that the model used here returns export flux at a fixed depth of 100 m, although export at the base of the euphotic layer has been suggested as an alternative metric [*Buesseler and Boyd*, 2009]. Recent model studies that use a variable export depth [*Siegel et al*., 2014; *Lima et al*., 2014] show similar spatial patterns of annual average export flux as here, although again the model used here overestimates export in a band at ~ 50°S. It should be noted that in this study using export flux from a fixed depth of 100 m results in an underestimate of export in productive regions and vice versa, relative to calculations made with a variable export depth.

Seasonally resolved in situ estimates of e-ratio are relatively sparse, particularly outside of the subtropics. However, the model compares favorably with data from the Hawaii Ocean Time Series site (HOTS) which show a seasonally invariant e-ratio of ~ 0.06 [*Brix et al*., 2006], whereas the model has somewhat more variability ranging from ~ 0.09 to 0.13. At BATS, the model overestimates e-ratio at ~ 0.18 compared to mean in situ values of ~ 0.07–0.11 although both model and data are seasonally invariant [*Buesseler*, 1998; *Brix et al*., 2006]. In the equatorial Pacific, observations suggest little change in e-ratio from spring to fall (~0.04–0.05) [*Buesseler et al*., 1995], and again, the model overestimates e-ratio (~0.09–0.14) but shows little seasonality. The Arabian Sea on the other hand has a distinct seasonal cycle linked to the monsoons and exhibits highest e-ratio in the late southwest monsoon with e-ratio increasing from ~ 0.02–0.05 to ~ 0.15–0.25 [*Buesseler*, 1998], comparable to the model which shows a similar seasonality, with e-ratio increasing from ~0.05–0.1 to ~0.2–0.32. At high latitudes, e-ratios in both observations and the model are generally higher. In the North Pacific, e-ratio increases from ~0.15 to 0.5 from April to July before declining again in autumn to ~0.06–0.25 [*Kawakami and Honda*, 2007]. The model has a similar seasonal pattern, although not as pronounced as in the observations, increasing from ~0.2 to 0.35 during spring/summer before declining to ~0.18–0.28 in autumn. Similarly, at the NABE site observations show an increase in e-ratio from 0.23 to 0.5 in spring, dropping off to 0.44 after the peak of the bloom [*Buesseler et al*., 1992]. The model follows this pattern although the seasonality is less pronounced, increasing from 0.21 to 0.3 before declining to 0.26. In the Bering Sea, observations of e-ratio [*Baumann et al*., 2013] show an increase from spring ($<$0.25) to summer (0.5), echoed in the model (from 0.2 to 0.4). Overall, the model reproduces the broad spatial and seasonal patterns found in observations, although with important caveats associated with its tendency to overestimate e-ratio in some low-latitude regions and underestimate the degree of seasonal variability at high latitudes.

3. Results

3.1. Spatial Variability in e-Ratio

Establishing a relationship between PP and e-ratio has enabled global-scale estimates of export efficiency to be derived from remotely sensed data. The most widely used relationship is that of *Laws et al*. [2000] which displays an exponential increase in e-ratio with increasing PP. This relationship was derived from just 11 in situ data points, the majority of which are in low-latitude regions. Conversely, a recent examination of export ratios in the Southern Ocean [*Maiti et al*., 2013] found an inverse relationship to that of *Laws et al*. [2000], with the e-ratio decreasing with increasing PP (data from *Maiti et al*. [2013] and additional observations from *Henson et al*. [2011] are plotted alongside the *Laws et al*. [2011] relationship in Figure 2c). These conflicting results suggest that the relationship between PP and export may be regionally variable and that simple empirical algorithms are not necessarily globally applicable.

We randomly subsampled the biogeochemical model in 1000 locations. The relationship between annual total PP and e-ratio is plotted in Figure 2a. In the model, e-ratio increases with increasing PP in warm regions and shows an inverse relationship (i.e., e-ratio increases with decreasing PP) in cold regions. There is a clear dichotomy in export efficiency at low PP between subtropical and subpolar regions: in subpolar regions ($<$ ~ 7°C), high export occurs at low PP, whereas in subtropical areas low PP conditions are associated with low export. The model therefore shows behavior that is similar to both the *Maiti et al*. [2013] and *Laws et al*. [2000] studies (Figure 2c), implying pronounced regional variability in the relationship between PP and e-ratio.

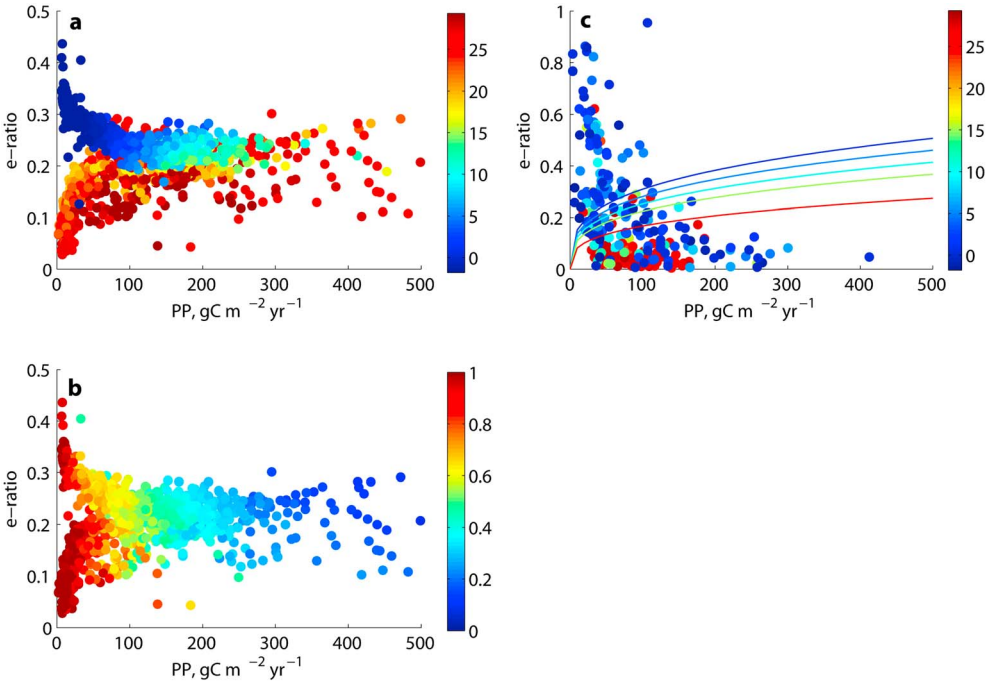

Figure 2. Modeled total annual primary production (PP) versus e-ratio, with points colored by (a) annual mean SST (°C) and (b) fraction of total annual export that is slowly sinking. (c) Observed PP versus e-ratio from a combination of data collated in *Maiti et al.* [2013] and *Henson et al.* [2011], colored by annual mean SST (dots). Also plotted is the empirically modeled relationship between PP and e-ratio calculated from *Laws et al.* [2011] using SST of 0, 5, 10, 15, and 25°C (lines).

The same plot with points colored according to the fraction of annual export that occurs as slow-sinking particles demonstrates that low PP is associated with a high proportion of slow-sinking export, which has opposing effects on e-ratio in high versus low latitudes (Figure 2b). In low latitudes the connection between a high proportion of slow-sinking export and low e-ratio is fairly intuitive; slowly sinking particles spend longer in the upper ocean and so can be rapidly remineralized at relatively shallow depths ($<$ 100 m) and therefore do not contribute to export. The reasoning for a high fraction of slowly sinking particles resulting in high export efficiency at high latitudes is perhaps less obvious. In these regions, annual mean SST is $<$ ~ 3°C. The model parameterizes remineralization as a function of temperature so that at these cold temperatures remineralization occurs very slowly. A relatively large proportion of slow-sinking particles are thus able to escape the upper ocean and contribute significantly to the export flux.

In the model's representation of the biological carbon pump, both temperature and the relative contribution of slow-sinking particles to export are critical factors in determining the export efficiency.

3.2. Lag Between Primary Production and Export

PP is unlikely to be converted instantaneously into sinking flux. Processes such as aggregation of individual particles until a sufficient density or size to sink is reached, or grazing by zooplankton and subsequent excretion as fecal pellets, must occur first. This time lag is difficult to quantify using in situ observations, partly because sampling programs do not cover the full seasonal cycle (with the exception of time series stations, such as BATS) and partly because the integration time scales of in situ PP and export measurements are usually mismatched. PP incubations typically last 12–24 h, whereas export estimates integrate over periods of a few days (e.g., Pelagra traps) [*Lampitt et al.*, 2008] to a few months (Pb/Po pair) [*Cochran and Masque*, 2003].

The model allows us to explore how temporal variability in PP and export are related, and how this is reflected in the e-ratio. The climatological annual cycle of PP, export, and corresponding e-ratio in both a strongly and weakly seasonal location are plotted in Figure 3. In the high-latitude Northwest Atlantic, modeled PP has pronounced seasonality with a single, extended peak in the summer months (Figure 3a). Peak export production lags PP by 20 days. The delay between PP increasing and a resultant increase in export is

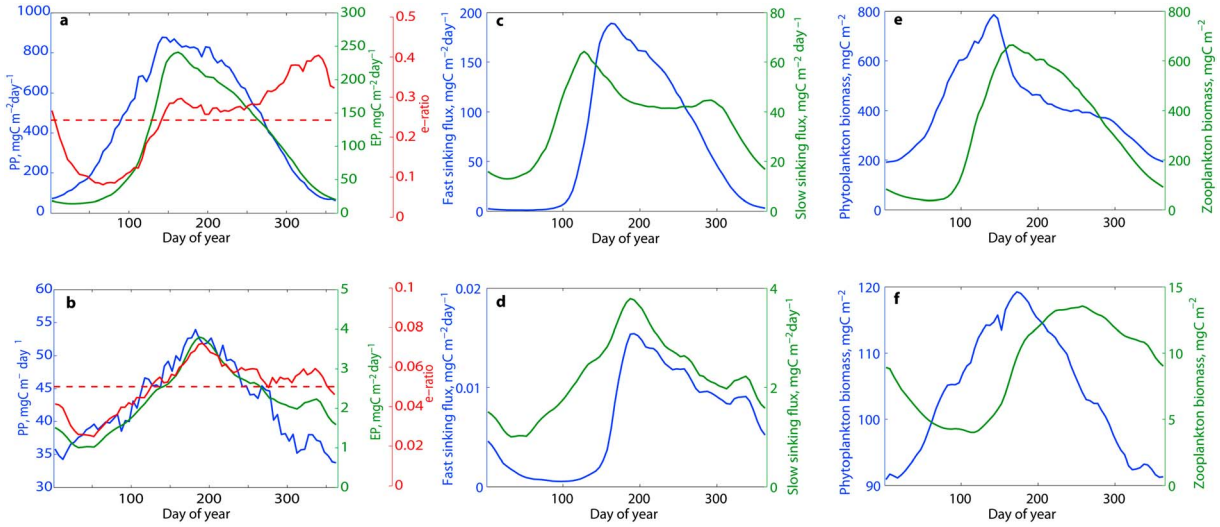

Figure 3. Annual time series of primary production (PP; blue), export production (EP; green), and e-ratio (red) at an example (a) subpolar location, 58°N, 35°W, and (b) subtropical location, 23°N, 58°W. Dotted red line indicates annual mean e-ratio. (c and d) Time series of fast-sinking (blue) and slow-sinking fluxes (green) at the same subpolar and subtropical locations, respectively. (e and f) Phytoplankton biomass (blue) and zooplankton biomass (green) at the same subpolar and subtropical locations, respectively. Note change of scale on *y* axis for subpolar and subtropical examples.

particularly pronounced at the start of the productive season (approximately March), when there is a lag of ~ 45 days. Consequently, the e-ratio is at its lowest in the spring as PP increases rapidly prior to the peak of the bloom. The e-ratio is relatively constant for a period of ~ 3 months after the peak of the bloom then increases in the autumn/winter as both PP and export decline, although at different rates. In the low-latitude western Atlantic, PP has very weak seasonality, with only a small increase above the mean in summer (Figure 3b). Export is equally nonseasonal but does, however, lag PP by 5 days. The e-ratio has a much lower variance than in the high-latitude example but has a similar pattern with a minimum prior to the peak PP.

Globally, the lagged correlation between annual time series of PP and export at each model grid point was calculated for all values of lag ranging from 0 to 40 days. The lag corresponding to the maximum correlation coefficient is plotted in Figure 4. The shortest lags of 0–10 days are found in upwelling regions and surrounding low-latitude areas (Benguela upwelling, equatorial Pacific, and Arabian Sea). The oligotrophic gyre edges and the Arctic tend to have the longest lags, of 30–40 days. Lags of 20–30 days are principally found in the Southern Ocean and North Atlantic, in contrast to the North Pacific which has lags of 10–15 days.

The degree of seasonal variability in a region is likely to be important in determining the lag between PP and export and therefore the seasonal variability in the e-ratio. The seasonal variation index of PP (standard deviation of PP/mean PP) is plotted against lag in Figure 5a and demonstrates that the lag between PP and export generally increases with increasing seasonality in PP up to a lag of 35 days. The seasonal variability in e-ratio also increases with increasing seasonality in PP (Figure 5b). PP is not necessarily exported immediately so that in high variability regions where PP can change rapidly, PP and export become decoupled, resulting in large seasonal variability in e-ratio. The implication is that estimates of e-ratio based on one-off in situ samples may be biased away from the annual mean depending on when in the seasonal cycle sampling occurs.

3.3. Seasonal Decoupling Between Primary Production and Export

Plots of modeled PP against export for the climatological year reveal seasonal decoupling. Model output from the same two example locations as in Figure 3 is plotted in Figure 6. If the e-ratio was seasonally invariant, points in Figure 6 would fall along a straight line. Instead, the e-ratio varies nonlinearly during the course of the year as PP and export become decoupled. This is more pronounced in the high-latitude example, where e-ratio varies from ~ 5% in winter to ~ 30% in spring and then increases again during autumn to a peak of ~ 40%. In the low-latitude example, e-ratio is less seasonally variable, although an increase from ~ 3 to 8% occurs during the summer period.

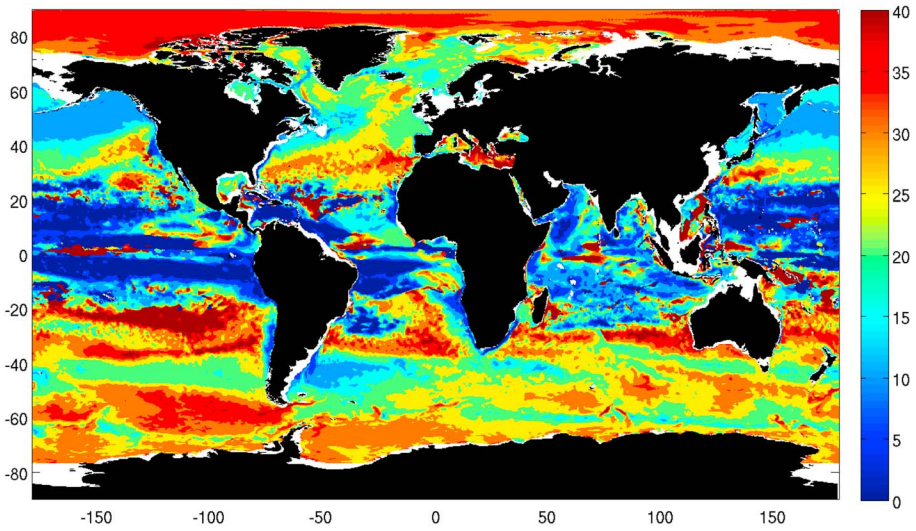

Figure 4. Lag in days between primary production and export production.

Because of the limited availability of observations, annual estimates of export are often extrapolated from instantaneous measurements of e-ratio [e.g., *Laws et al.*, 2000; *Henson et al.*, 2011], which makes the implicit assumption that the instantaneous e-ratio is representative of the annual mean. The effect that the seasonal decoupling has on the estimation of annual export is demonstrated in Figure 7, which shows the percentage difference from the model annual total export when calculated using the e-ratio 1 month prior to peak PP, at the time of peak PP, and 1 month after peak PP and making a "steady state" assumption, i.e., that the instantaneous e-ratio at that time is representative of the annual mean. (Note that values

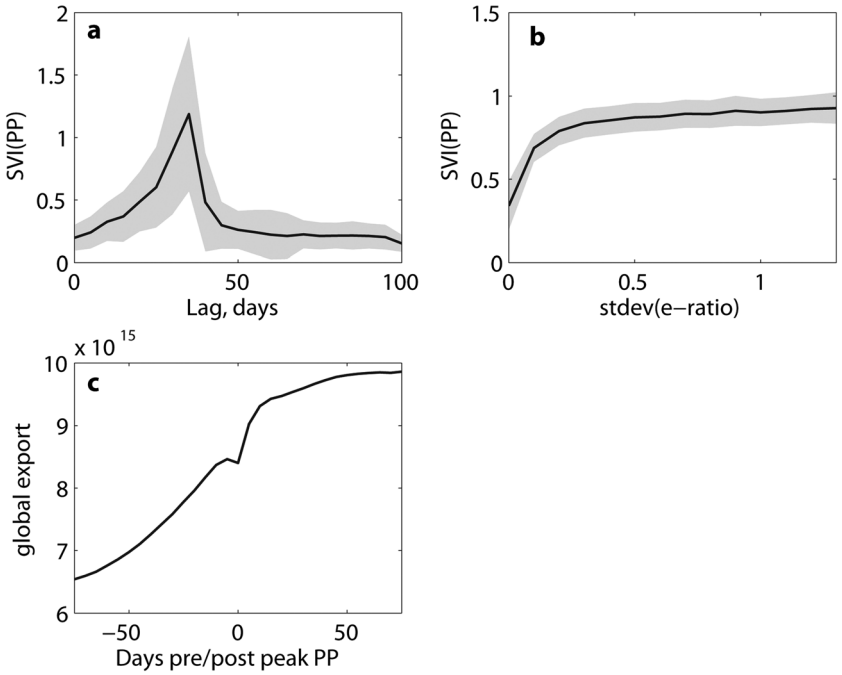

Figure 5. Global averages (black lines) and standard deviation (grey bands) showing relationships between (a) lag between primary production (PP) and export and seasonal variation index (SVI) of PP (standard deviation of PP/mean PP), (b) standard deviation in e-ratio within 1 year and SVI of PP, and (c) global annual export (gC) calculated using e-ratio values up to 75 days before and after peak PP.

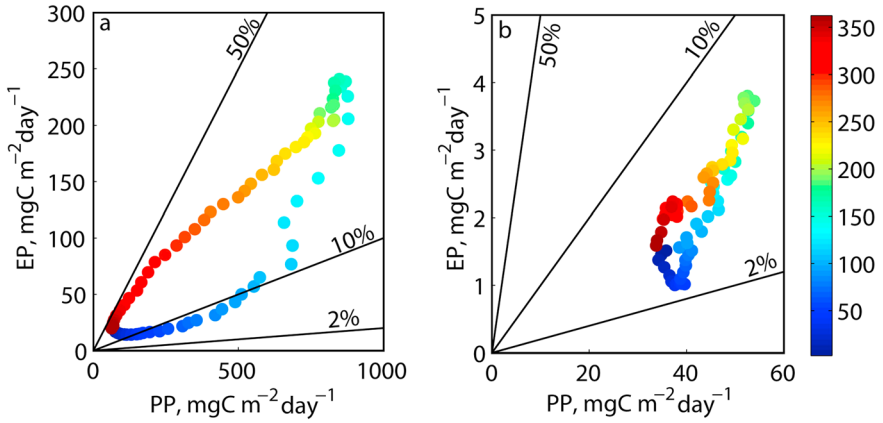

Figure 6. Annual evolution of primary production (PP) and export production (EP) at an example (a) subpolar location, 58°N, 35°W, and (b) subtropical location, 23°N, 58°W. Points are colored by day of year. Straight lines indicate e-ratios of 0.02, 0.1, and 0.5. Note different scales for subpolar and subtropical examples.

are identical for the percentage difference between instantaneous e-ratio and the annual mean e-ratio.) In the majority of locations, annual export estimates extrapolated from instantaneous measurements made 1 month before peak PP are lower by ~ 20–60% than the true annual total export. Exceptions occur in the North Pacific and along subpolar boundary regions in the North Atlantic and Southern Ocean where scaling up instantaneous export overestimates annual total export by < 20%. In equatorial regions, the results are patchy with areas of both underestimation and overestimation of < ± 20%. When annual export is extrapolated from measurements taken at peak PP, subpolar regions tend to overestimate export by ~ 5–50%, while in the gyres, annual export is underestimated by ~ 5–40%. Finally, if annual export

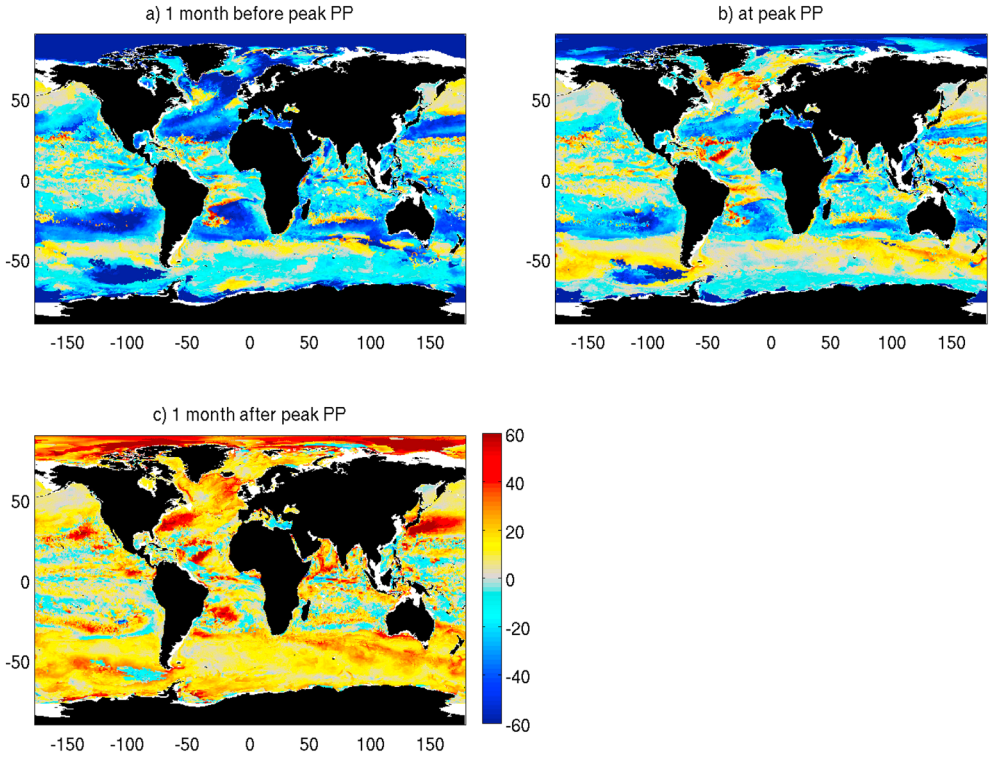

Figure 7. Percentage difference in annual total export when calculated assuming steady state and using e-ratio (a) 1 month prior to peak PP, (b) at peak PP and (c) 1 month after peak PP, compared to true model total export.

is calculated assuming that export 1 month after peak PP is representative of the annual total, export is overestimated almost everywhere by up to 60%. Thus, the steady state assumption that instantaneous measurements of export can be scaled up to estimate annual total export can result in large errors due to seasonal variability in the export and e-ratio. The largest differences are found in highly seasonal locations, such as the subpolar North Atlantic, i.e., regions which are frequently targeted for in situ export studies.

3.4. Role of Trophic Coupling

In the model, fast-sinking detrital particles are generated by losses of diatoms and egestion by mesozooplankton. These particles do not "sink" per se but are instantly (within the time step of the model) remineralized down the water column, with the shape of the remineralization curve driven by a ballast model [*Armstrong et al*., 2002]. Slowly sinking particles derive from the nondiatom population and sink at an explicit rate of $3\ m\ d^{-1}$. Thus, in contrast to the fast-sinking particles, this material is not exported immediately but is instead consumed by both microzooplankton and mesozooplankton and remineralized at a rate dependent on ambient temperature. The effect of this is demonstrated in Figures 3c and 3d and Figures 3e and 3f which show the annual time series of slow- and fast-sinking export fluxes alongside the total phytoplankton (diatom + nondiatom) and zooplankton (meso + micro) biomass at an example subpolar and subtropical location. In the subpolar location, phytoplankton biomass increases rapidly in spring as their growth rate exceeds that of zooplankton. Only slow-sinking particles are produced at this stage, and the lag between PP and export is large as a result. As zooplankton biomass increases so too does the fast-sinking flux, which is reflected in increased export. As phytoplankton and zooplankton biomass become more closely coupled in the postbloom phase, so the lag between PP and export decreases. In the subtropical region, the slow-sinking fraction dominates the total export flux throughout the year. The seasonal range of phytoplankton and zooplankton biomass is very small, not undergoing any large seasonal excursions away from the annual mean, resulting in little lag between PP and export. Thus, in the model the lag between PP and export arises principally due to the seasonal decoupling between primary producers and their consumers, and the concomitant production of slow- and fast-sinking particles, respectively.

4. Discussion

Several empirical models to estimate global export on the basis of remotely sensed parameters, such as SST, PP, or chlorophyll have been developed [*Laws et al*., 2000, 2011; *Dunne et al*., 2005; *Henson et al*., 2011]. These are derived from databases of in situ measurements which are necessarily sparsely distributed, both spatially and temporally, and are biased toward summer periods and the Northern Hemisphere. The implications of this sampling bias for interpreting isolated measurements of e-ratio and for extrapolating to larger scales are investigated here using a global biogeochemical model.

A commonly used algorithm for estimating export is the food web model of *Laws et al*. [2000] which predicts a nonlinear *increase* in e-ratio with increasing PP. This directly contradicts a recently published compilation of Southern Ocean data that demonstrates a nonlinear *decrease* in e-ratio with increasing PP [*Maiti et al*., 2013] (see also Figure 2c). These opposing results suggest that regional differences in the relationship between PP and e-ratio may exist. The biogeochemical model supports this supposition—warm and cold regions differ significantly in their e-ratios at low PP (Figure 2). The divergence in the relationship is associated with a high proportion of slow-sinking export flux, the remineralization of which is temperature controlled. In very cold regions ($< \sim 3$°C), remineralization is so retarded that a relatively large fraction of material, even if slowly sinking, can be exported. In warm regions, however, rapid remineralization of the slow-sinking fraction results in low e-ratio at low PP. These results imply that simple empirical algorithms to estimate export ratios and designed to be applied globally may be an oversimplification.

One potential difficulty in developing empirical algorithms for e-ratio or export from databases of in situ measurements is that sampling captures a temporally and spatially limited snapshot of the system. Using these samples to estimate total annual export (as is done in, for example, *Laws et al*. [2000]; *Henson et al*. [2011], and *Dunne et al*. [2005]) implicitly makes the necessary assumption that the instantaneous measurements represent the annual mean, i.e., that the e-ratio does not change seasonally. This steady state assumption is necessary because very little data on the seasonal variability in e-ratio is available as it requires regularly repeated ship-based sampling (although see information on seasonally resolved e-ratio observations in section 2).

The model suggests that the lag between PP and export can drive large excursions ($> \pm 60\%$) of the instantaneous e-ratio away from the annual mean. This seasonal variability in e-ratio is largest in regions of high seasonal variability in PP, as might be expected from consideration of the model's ecosystem dynamics. In highly seasonal locations, diatoms grow rapidly and outpace their grazers who have a slower growth rate. The export of material is limited at this stage until the grazing population begin to consume the primary producers in earnest at which point exported matter in the form of sinking PP and mesozooplankton excretion increases rapidly (e.g., Figures 3c and 3e). Toward the end of the bloom, PP declines as resources become limited and grazing regulates the population, but export continues in the form of microzooplankton and mesozooplankton excretion. The lag between PP and export is greatest in seasonally variable, i.e., bloom-forming, regions, which results in an e-ratio lower (greater) than the mean prior to (after) peak PP. At low latitudes, lags are noticeably shorter, suggesting a tighter coupling between producers and grazers, resulting in less variability in e-ratio (e.g., Figures 3b and 3f). In the high-latitude North Pacific, lags are ~ 10–15 days compared to similar latitudes in the North Atlantic where lags are ~ 20–30 days, consistent with the hypothesis that zooplankton exert a greater control over phytoplankton populations in the subpolar Pacific than Atlantic Oceans [*Frost*, 1987]. The model clearly suggests that the steady state assumption is not valid, particularly in strongly seasonal regions.

The effects of decoupling between phytoplankton and zooplankton populations have been previously suggested as a mechanism for generating seasonal variability in e-ratio [e.g., *Buesseler*, 1998; *Wassmann*, 1998]. Although relatively few seasonally resolved coincident estimates of PP and export flux have been made, a general pattern emerges. In low-latitude regions, there is typically little seasonality in PP or export flux [*Buesseler*, 1998; *Owens et al*., 2013], indicative of a tightly coupled food web. E-ratio is relatively seasonally invariant, as shown in *Brix et al*. [2006] where a plot of seasonal average PP versus export at station ALOHA shows a linear relationship, i.e., near constant e-ratio (their Figure 2f, compare to our Figure 6b). In contrast, high-latitude regions tend to have strong seasonality in PP which is reflected in the export flux, implying a degree of decoupling between phytoplankton and zooplankton in bloom situations [e.g., *Kawakami and Honda*, 2007; *Buesseler et al*., 2009; *Baumann et al*., 2013]. Seasonally resolved data from a Norwegian fjord demonstrated this decoupling [*Wassmann*, 1998], with a plot of PP versus export showing a large loop, i.e., highly variable e-ratio (their Figure 19a, compare to our Figure 6a), which was interpreted as a mismatch between phytoplankton and zooplankton populations. The examples plotted in Figure 6 are strongly reminiscent of the in situ data of *Brix et al*. [2006] and *Wassmann* [1998]; in the subtropical example, the seasonal evolution of e-ratio is approximately linear, whereas in the subpolar location, e-ratio follows a looped trajectory during the course of a year.

The large excursions in e-ratio away from the mean predicted here by the model have significant implications for the interpretation of in situ data, particularly measurements that do not represent a time series (i.e., the vast majority of export measurements). Our results suggest that the interpretation of in situ e-ratio estimates should be undertaken in the context of the seasonal cycle of productivity in that region, i.e., is the measurement representative of prebloom, peak, or postbloom conditions? In the majority of cases, establishing when in the seasonal cycle measurements were taken will require satellite-derived chlorophyll or PP data, as the only source of spatially and temporally resolved information. Establishing causal links between variability in e-ratio and potential drivers, e.g., phytoplankton community structure, is also confounded by the lag between PP and export. A change in the ecosystem structure may have a rapid effect on PP, but a corresponding change in export may not occur until days to weeks later, dissociating the driver and response. Care is therefore needed in interpreting sparse in situ estimates of e-ratio, particularly if an implicit assumption is being made that the instantaneous estimate is representative of a longer-term mean.

The potential effect of the steady state assumption on globally integrated export estimates can be illustrated by comparing the export derived from sampling the model at different stages prior to and post peak PP to the true annual model export. In Figure 5c, the global total export calculated from sampling the model up to 75 days prepeak/postpeak PP and making the steady state assumption is plotted. Globally averaged, the difference ranges from an underestimate of ~ 25% 75 days prior to peak PP to an overestimate of ~ 15% 75 days after peak PP. This equates to a range of 6.5–10 Pg C yr^{-1} around the true model value of 8.5 Pg C yr^{-1}.

Current estimates of global carbon export range from ~ 5 to 12 Pg C yr^{-1} [*Henson et al*., 2011], with the majority of estimates clustered around 10–12 Pg C yr^{-1}. These estimates are derived from databases of

export or export ratio from a variety of measurement techniques, including ^{234}Th disequilibria, ^{15}N uptake ratios, and shallow sediment traps, which are then correlated with a remotely sensed proxy (usually SST and/or chlorophyll) to produce a global estimate. One possible explanation for the discrepancy between estimates is the influence that sparsely distributed data (biased toward the Northern Hemisphere and spring/summer) may have on the derived global estimates. The range in global export calculated above on the basis of prebloom versus postbloom sampling is 3.5 Pg C yr^{-1}, half of the range in the data-derived estimates (7 Pg C yr^{-1}) [*Laws et al*., 2000; *Henson et al*., 2011]. This suggests that a substantial proportion of the uncertainty in global export estimates could arise from differences in the space/time distribution of samples, although this is clearly not the only source of the discrepancies. One of the lowest estimates of global export comes from a database of ^{234}Th-derived export measurements [*Henson et al*., 2011; *Le Moigne et al*., 2013] in which the majority of samples were taken in the bloom peak or postbloom period. Our results here suggest that this should lead to an overestimate of annual export, which would widen further the difference between the thorium-based estimate and those of, e.g., *Laws et al*. [2000] and *Schlitzer* [2000]. As such, the root cause of the large discrepancy between the thorium-based estimate and others is therefore probably not differences in the spatial and temporal distribution of sampling, but rather some difference in the operation of the measurement techniques. For example, thorium-derived export is calculated after filtering samples through a 53 μm screen and so is only capturing the flux of large particles [*Buesseler et al*., 2006]. Recent observational studies have confirmed that the small, slower-sinking fraction may also be a significant component of the total flux [*Alonso-Gonzalez et al*., 2010; *Riley et al*., 2012], a suggestion supported by the model results presented here (e.g., Figure 3d).

A key caveat to the results presented here is that they are derived from a single biogeochemical model, MEDUSA, and the results are therefore necessarily dependent on the structure and parameterization of this model. MEDUSA explicitly divides the spectrum of sinking particles into two pools with fixed sinking rates and makes assumptions concerning the production, remineralization, and function of both pools within the food web. This parameterization of marine detrital pools permits the time lags between PP and export investigated here to develop and, although we believe this behavior to be realistic and the parameterizations are based on field data, clearly the details of the calculated lags and errors in export due to the steady state assumption depend on the model formulation. Other models that include alternative parameterizations of slow- and fast-sinking particles or do not make that distinction and have only one pool of sinking material, may well exhibit different behavior. Furthermore, the model does have some limitations associated with its parameterization. For example, the model results suggest that slow-sinking particles can, in some locations, make up 100% of the export flux (Figure 1d), although this has not yet been observed in situ. A fixed sinking speed for slow particles of 3 m d^{-1} is also used, although observations suggest that sinking speed may change seasonally and with depth [*Trull et al*., 2008; *McDonnell and Buesseler*, 2010]. In addition, the model does not include processes such as coagulation of aggregates, disaggregation of particles, or details of microbial food web dynamics that may be important in determining lags between particle production and export [*Jackson*, 2001; *Legendre and Lefevre*, 1995]. Finally, export flux through a fixed depth horizon (100 m) is used here; however, an alternative is to estimate export at a variable depth (typically the base of the euphotic zone [*Buesseler and Boyd*, 2009]). This constraint in the model likely results in an underestimate of export flux in productive regions or periods and vice versa. This would tend to enhance further the decoupling and offsets shown here.

Despite these caveats, the model simulates behavior seen in the observations, both in the relationship between e-ratio and SST (Figures 2a and 2c) and in the seasonal decoupling between PP and export (Figure 6) and so is a useful tool for exploring when, where, and how variability in e-ratio arises. The model thus provides a stimulus to consider how seasonal variability might alter in situ estimates of the e-ratio and how this might carry through to "errors" in global export calculations. Testable hypotheses have also arisen from this model study that could be examined using either existing data or through targeted sampling. For example, the biogeochemical model suggests that the proportion of slow-sinking particles influences the divergence in e-ratio in warm and cold regions at low PP (Figure 2b). The contribution of slow-sinking particles to total export has not been frequently quantified observationally, although instruments such as the Marine Snow Catcher [*Riley et al*., 2012] and the Indented Rotating Sphere [*Alonso-Gonzalez et al*., 2010] can provide information on fluxes separated by sinking speed. The hypotheses suggested by the model results thus await testing through a compilation of sinking speed-differentiated export fluxes.

Our results, admittedly based solely on a biogeochemical model, make a strong case for establishing in situ time series of seasonal variability in e-ratio, particularly in highly seasonal regions. This is technically challenging as repeat measurements of PP and export are required. PP may be estimated from satellite data, but export, particularly if slow/fast pools are to be distinguished, must be measured in situ. Shallow traps, if not operated in a Lagrangian mode, do not provide accurate measures of export due to swimmers, advection, and undertrapping. Current ship-serviced time series stations, such as BATS and HOTS, can offer high-quality, repeat measurements but are in weakly seasonal regions; however, ship-serviced time series stations in high-latitude regions would present a raft of logistical problems. Technological developments, such as the Carbon Flux Explorer [*Bishop and Wood*, 2009] may provide some indication of flux variability although, as with Lagrangian floats, their mode of operation adds a degree of complexity when interpreting the resulting data as a time series. Although challenging to acquire, more time series of export flux would allow testing of the hypotheses suggested here and potentially lead to improved algorithms for estimating e-ratio from remotely sensed data and thus both more accurate estimates of global carbon export and more realistically parameterized models.

Acknowledgments
This work was supported by NERC grant NE/J004383/1 to S.A.H. Many thanks to Kanchan Maiti for supplying data for Figure 2c. Output from this run of the NEMO-MEDUSA model can be obtained on application to the authors (contact s.henson@noc.ac.uk and axy@noc.ac.uk).

References

Alonso-Gonzalez, I. J., J. Aristegui, C. Lee, A. Sanchez-Vidal, A. Calafat, J. Fabres, P. Sangra, P. Masque, A. Hernandez-Guerra, and V. Benitez-Barrios (2010), Role of slowly settling particles in the ocean carbon cycle, *Geophys. Res. Lett.*, *37*, L13608, doi:10.1029/2010GL043827.

Armstrong, R. A., C. Lee, J. I. Hedges, S. Honjo, and S. G. Wakeham (2002), A new, mechanistic model for organic carbon fluxes in the ocean based on the quantitative association of POC with ballast minerals, *Deep Sea Res., Part II*, *49*(1–3), 219–236.

Baumann, M. S., S. B. Moran, M. W. Lomas, R. P. Kelly, and D. W. Bell (2013), Seasonal decoupling of particulate organic carbon export and net primary production in relation to sea-ice at the shelf break of the eastern Bering Sea: Implications for off-shelf carbon export, *J. Geophys. Res. Oceans*, *118*, 5504–5522, doi:10.1002/jgrc.20366.

Behrenfeld, M. J., and P. G. Falkowski (1997), Photosynthetic rates derived from satellite-based chlorophyll concentration, *Limnol. Oceanogr.*, *42*(1), 1–20.

Benitez-Nelson, C., K. O. Buesseler, D. M. Karl, and J. Andrews (2001), A time-series study of particulate matter export in the North Pacific Subtropical Gyre based on Th-234: U-238 disequilibrium, *Deep Sea Res., Part I*, *48*(12), 2595–2611.

Bishop, J. K. B., and T. J. Wood (2009), Year-round observations of carbon biomass and flux variability in the Southern Ocean, *Global Biogeochem. Cycles*, *23*, GB2019, doi:10.1029/2008GB003206.

Brix, H., N. Gruber, D. M. Karl, and N. R. Bates (2006), On the relationships between primary, net community, and export production in subtropical gyres, *Deep Sea Res., Part II*, *53*, 698–717.

Buesseler, K. O. (1998), The decoupling of production and particulate export in the surface ocean, *Global Biogeochem. Cycles*, *12*(2), 297–310, doi:10.1029/97GB03366.

Buesseler, K. O., and P. W. Boyd (2009), Shedding light on processes that control particle export and flux attenuation in the twilight zone of the open ocean, *Limnol. Oceanogr.*, *54*, 1210–1232.

Buesseler, K. O., M. P. Bacon, J. K. Cochran, and H. D. Livingston (1992), Carbon and nitrogen export during the JGOFS North-Atlantic Bloom Experiment estimated from Th-234:U-238 disequilibria, *Deep Sea Res.*, *39*(7–8A), 1115–1137.

Buesseler, K. O., J. Andrews, M. C. Hartman, R. Belastock, and F. Chai (1995), Regional estimates of the export flux of particulate organic carbon derived from Th-234 during the JGOFS EqPac program, *Deep Sea Res., Part II*, *42*(2–3), 777–791.

Buesseler, K. O., et al. (2006), An assessment of particulate organic carbon to thorium-234 ratios in the ocean and their impact on the application of Th-234 as a POC flux proxy, *Mar. Chem.*, *100*, 213–233.

Buesseler, K. O., S. Pike, K. Maiti, C. H. Lamborg, D. A. Siegel, and T. W. Trull (2009), Thorium-234 as a tracer of spatial, temporal and vertical variability in particle flux in the North Pacific, *Deep Sea Res., Part A*, *56*, 1143–1167.

Carr, M. E., et al. (2006), A comparison of global estimates of marine primary production from ocean color, *Deep Sea Res., Part II*, *53*, 741–770.

Cochran, J. K., and P. Masque (2003), Short-lived U/Th series radionuclides in the ocean: Tracers for scavenging rates, export fluxes and particle dynamics, in *Uranium-Series Geochemistry*, edited by B. Bourdon et al., pp. 461–492, Mineral. Soc. Am., Chantilly, Va.

DRAKKAR Group (2007), Eddy permitting ocean circulation hindcasts of past decades, *Clivar Exchanges*, *42*, 8–10.

Dunne, J. P., R. A. Armstrong, A. Gnanadesikan, and J. L. Sarmiento (2005), Empirical and mechanistic models for the particle export ratio, *Global Biogeochem. Cycles*, *19*, GB4026, doi:10.1029/2004GB002390.

Dunne, J. P., J. L. Sarmiento, and A. Gnanadesikan (2007), A synthesis of global particle export from the surface ocean and cycling through the ocean interior and on the seafloor, *Global Biogeochem. Cycles*, *21*, GB4006, doi:10.1029/2006GB002907.

Falkowski, P. G., R. T. Barber, and V. Smetacek (1998), Biogeochemical controls and feedbacks on ocean primary production, *Science*, *281*(5374), 200–206.

Frost, B. W. (1987), Grazing control of phytoplankton stock in the open sub-arctic Pacific-Ocean—A model assessing the role of mesozooplankton, particularly the large calanoid copepods Neocalanus spp, *Mar. Ecol. Prog. Ser.*, *39*(1), 49–68.

Henson, S. A., R. Sanders, E. Madsen, P. J. Morris, F. Le Moigne, and G. D. Quartly (2011), A reduced estimate of the strength of the ocean's biological carbon pump, *Geophys. Res. Lett.*, *38*, L04606, doi:10.1029/2011GL046735.

Jackson, G. A. (2001), Effect of coagulation on a model planktonic food web, *Deep Sea Res., Part A*, *48*(1), 95–123, doi:10.1016/s0967-0637(00)00040-6.

Kawakami, H., and M. C. Honda (2007), Time-series observation of POC fluxes estimated from (234) Th in the Northwestern North Pacific, *Deep Sea Res., Part A*, *54*, 1070–1090.

Kwon, E. Y., F. Primeau, and J. L. Sarmiento (2009), The impact of remineralization depth on the air-sea carbon balance, *Nat. Geosci.*, *2*, 630–635.

Lampitt, R. S., B. Boorman, L. Brown, M. Lucas, I. Salter, R. Sanders, K. Saw, S. Seeyave, S. J. Thomalla, and R. Turnewitsch (2008), Particle export from the euphotic zone: Estimates using a novel drifting sediment trap, Th-234 and new production, *Deep Sea Res., Part A*, *55*, 1484–1502.

Large, W., and S. Yeager (2004), Diurnal to decadal global forcing for ocean and sea ice models: The data sets and flux climatologies, *Tech. Note NCAR/TN-460+STR*.

Laws, E. A., P. G. Falkowski, W. O. Smith, H. Ducklow, and J. J. McCarthy (2000), Temperature effects on export production in the open ocean, *Global Biogeochem. Cycles*, *14*(4), 1231–1246, doi:10.1029/1999GB001229.

Laws, E. A., E. D'Sa, and P. Naik (2011), Simple equations to estimate ratios of new or export production to total production from satellite-derived estimates of sea surface temperature and primary production, *Limnol. Oceanogr. Methods*, *9*, 593–601.

Le Moigne, F., S. A. Henson, R. Sanders, and E. Madsen (2013), Global database of surface ocean particulate organic carbon export fluxes diagnosed from the ^{234}Th technique, *Earth Syst. Sci. Data*, *5*, 295–304.

Le Quere, C., et al. (2013), The global carbon budget 1959–2011, *Earth Syst. Sci. Data*, *5*, 165–185.

Legendre, L., and J. Lefevre (1995), Microbial food webs and the export of biogenic carbon in oceans, *Aquat. Microb. Ecol.*, *9*(1), 69–77.

Lima, I. D., P. J. Lam, and S. C. Doney (2014), Dynamics of particulate organic carbon flux in a global ocean model, *Biogeosciences*, *11*, 1177–1198, doi:10.5194/bg-11-1177-2014.

Lutz, M. J., K. Caldeira, R. B. Dunbar, and M. Behrenfeld (2007), Seasonal rhythms of net primary production and particulate organic carbon flux to depth describe the efficiency of biological pump in the global ocean, *J. Geophys. Res.*, *112*, C10011, doi:10.1029/2006JC003706.

Maiti, K., M. A. Charette, K. O. Buesseler, and M. Kahru (2013), An inverse relationship between production and export efficiency in the Southern Ocean, *Geophys. Res. Lett.*, *40*, 1557–1561, doi:10.1002/grl.50219.

McDonnell, A. M. P., and K. O. Buesseler (2010), Variability in the average sinking velocity of marine particles, *Limnol. Oceanogr.*, *55*, 2085–2096.

Moran, S. B., M. W. Lomas, R. P. Kelly, R. Gradinger, K. Iken, and J. T. Mathis (2012), Seasonal succession of net primary productivity, particulate organic carbon export and autotrophic community composition in the eastern Bering Sea, *Deep Sea Res., Part II*, *65–70*, 84–97.

Owens, S. A., K. O. Buesseler, C. H. Lamborg, J. Valdes, M. W. Lomas, R. J. Johnson, D. K. Steinberg, and D. A. Siegel (2013), A new time series of particle export from neutrally buoyant sediments traps at the Bermuda Atlantic time-series study site, *Deep Sea Res., Part A*, *72*, 34–47.

Raven, J. A., and P. G. Falkowski (1999), Oceanic sinks for atmospheric CO_2, *Plant, Cell Environ.*, *22*(6), 741–755.

Riley, J. S., R. Sanders, C. Marsay, F. A. C. Le Moigne, E. P. Achterberg, and A. J. Poulton (2012), The relative contribution of fast and slow sinking particles to ocean carbon export, *Global Biogeochem. Cycles*, *26*, GB1026, doi:10.1029/2011GB004085.

Sabine, C. L., et al. (2004), The oceanic sink for anthropogenic CO_2, *Science*, *305*, 367–371.

Schlitzer, R. (2000), Applying the adjoint method for global biogeochemical modeling, in *Inverse Methods in Global Biogeochemical Cycles*, edited by P. Kasibhatla et al., pp. 107–124, AGU, Washington, D. C.

Siegel, D. A., K. O. Buesseler, S. C. Doney, S. F. Sailley, M. Behrenfeld, and P. W. Boyd (2014), Global assessment of ocean carbon export by combining satellite observations and food-web models, *Global Biogeochem. Cycles*, *28*, 181–196, doi:10.1002/2013GB004743.

Trull, T. W., S. G. Bray, K. O. Buesseler, C. H. Lamborg, S. Manganini, C. Moy, and J. Valdes (2008), In situ measurement of mesopelagic particle sinking rates and the control of carbon transfer to the ocean interior during the Vertical Flux in the Global Ocean (VERTIGO) voyages in the North Pacific, *Deep Sea Res., Part II*, *55*, 1684–1695.

Wassmann, P. (1998), Retention versus export food chains: Processes controlling sinking loss from marine pelagic systems, *Hydrobiologia*, *363*, 29–57.

Westberry, T., M. J. Behrenfeld, D. A. Siegel, and E. Boss (2008), Carbon-based primary productivity modeling with vertically resolved photoacclimation, *Global Biogeochem. Cycles*, *22*, GB2024, doi:10.1029/2007GB003078.

Yool, A., E. E. Popova, and T. R. Anderson (2011), Medusa-1.0: A new intermediate complexity plankton ecosystem model for the global domain, *Geosci. Model Dev.*, *4*, 381–417, doi:10.5194/gmd-4-381-2011.